DOI: https://doi.org/10.25202/JAKG.9.2.3 한국지리학회지 9권 2호 2020(265~279)

Understanding the Transport Mechanism of Paleo-deposits in the Sonoran Desert with Grain Size Distribution and Shape Analysis

Ara Jeong*

입자 크기와 입자 형상 분석을 통해 살펴본 소노란 사막 고퇴적층의 형성과정

정아라*

Abstract : About tens of meters thick fine sand and silt deposits are observed at the top of the sedimentary logs of hundreds of drilling wells throughout Phoenix metropolitan area, Arizona, USA, situated in north-central Sonoran Desert, and likely deposited after ~ 836ka. A hypothesis to explain the paleo-deposits is that the deposits are a wind-blown deposits derived from the floodplains of nearby rivers developed in response to the aeolian-fluvial interactions. The purpose of this study is to reconstruct paleoenvironment and to understand the processes of transport and deposition of the paleo-deposits using modern analogues. This is accomplished via the identification of the paleo-deposits by comparison with modern source-bordering dune sediments and fluvial sediments using the analyses of grain size distribution and grain shape parameters. Overall, the results of sediment drift potential, grain size distribution and shape analyses provide evidence to support the hypothesis, and the deposition of the paleo-deposits may be related with the change of regional climates. Grain shape parameters may better reflect the mechanism of transport when grains traveled over short distance. Given the advantage, the grain shape analysis may provide a new insight to solve the issue associated with the provenance of Korean loess-like sediments whether it was originated from far-distant the Chinese Loess Plateau and peripheral areas or from nearby floodplains of local river or from exposed fine materials in the Yellow Sea.
Key Words : Aeolian-fluvial interaction, Arid landform, Source-bordering dune, Grain size distribution, Grain shape analysis

요약 : 미국 소노란 사막에 위치한 애리조나 주 피닉스 시 일대의 수백 개 천공정의 최상부층에서 최대84만년 전 이후로 퇴적되었을 것으로 추정되는 수십 미터 두께의 가는 모래와 실트로 이루어진 고퇴적층이 발견되었다. 본 연구에서는 소노란 사막 내륙에서 형성된 고퇴적층이 주변 범람원으로부터 물질을 공급받아 풍성작용에 의해 퇴적되어 형성되었을 것이라는 가설을 세우고, 전통적으로 논의되어 온 건조지역의 지형 발달 프로세스를 "풍성-하성" 프로세스의 복합 요인으로 새롭게 조명하여 단거리 이동과 퇴적 가능성을 밝히고자 하였다. 이를 위해 현생 퇴적물 시료와 고퇴적층 시료에 대한 입도 분석과 입자 형상 분석을 수행한 결과, 전반적으로 해당 가설을 지지하는 것으로 나타났으며, 해당 고퇴적층의 형성과정에 소노란 사막 지역의 기후 변화가 작용하였을 것으로 생각된다. 한편, 본 연구는 입자 형상 분석이 단거리 이동 퇴적층의 형성과정을 규명하는데 있어 더 효과적인 방법일 수 있음을 보여주며, 이는 오랜 한국 지리학계의 논쟁이었던 뢰스와 같은 퇴적층의 형성과정과 기원지에 대한 연구에 새로운 가능성을 제시한다.
주요어 : 바람-하천 상호작용, 건조 지형, 공급지-경계 사구, 입도 분석, 입자 형상 분석

*고려대학교 지리교육과 연구교수(Research Professor, Department of Geography Education, Korea University, ara0408@korea.ac.kr)

I. Introduction

Loess-like sediments that was likely deposited by aeolian processes has been observed throughout Korea (e.g. Park, 1985; Oh and Kim, 1994; Kim, 2007; Yoon *et al.*, 2007; 2012; 2013; Park *et al.*, 2014), but the provenances of Korean loess have been debated. Some studies argued that Korean loess was likely originated from the Chinese Loess Plateau and peripheral areas (Park *et al.*, 2007; Yoon *et al.*, 2007; Hwang *et al.*, 2009), but others suggested that it was locally transported from floodplains of local river or from exposed fine materials in the Yellow Sea (Oh and Kim, 1994; Kim, 2007). In many inland drylands, source-bordering dunes are one of the most common landforms, representing a dune closely bordering its aeolian sediment source such as flood deposits of rivers (Page, 1971; Page *et al.*, 2001). Prolonged aridity lead to subaerial exposure of fluvial sediments, which more likely allow winds to entrain and transport these sediments depending on wind velocity and grain size (Jeong *et al.*, 2018). In certain places, the relationship between fluvial sediment source and aeolian deposits was observed even tens to hundreds of kilometers downwind of a river (Muhs *et al.*, 2003; Alizai *et al.*, 2011). Therefore, the interaction between aeolian and fluvial processes can play an important role in shaping arid landscapes (Bullard and Livingstone, 2002), but their interaction and links are rarely studied, except a couple of pioneering works (Bullard and Livingstone, 2002; Belnap *et al.*, 2011).

The study area, Phoenix metropolitan area, is in Köppen-Geiger warm desert (BWh) settings where mean annual precipitation is averaging about 200mm, winter daytime temperatures are in the lower 15°C and summer daytime temperatures are between 41°C and 46°C (Arizona State Climatologists office, https://azclimate.asu.edu). Phoenix metropolitan area is situated within the Sonoran Desert in the Basin and Range Province, and occupy low-relief areas in front of mountain ranges that includes the distal ends of pediments and alluvial fans, aeolian sand sheets, and alluvial deposits (Fig. 1) (Jeong *et al.*, 2018). A better understanding of contemporary aeolian-fluvial interactions can provide useful modern analogues that assists to interpret the paleoenvironmental history from stratigraphic record (Bullard and Livingstone, 2002), which can certainly apply to the Phoenix metropolitan area. Extensive areas near the Gila River traversing the Phoenix metropolitan are covered by source-bordering dunes or sand sheets (Fig. 1 and Fig. 2) and four eolian depositional events were identified from the trenches (~ 2m depth) in the Gila River dune fields during the late Holocene that reflect the aeolian-fluvial interactions (Wright *et al.*, 2011). This kind of massive fine sand and silt deposits (~ 73m depth) has also been identified from ample well drill-log data in the East Salt River Valley Sub-basin (Fig. 3), presenting an opportunity to understand the paleoenvironmental history. Hundreds of wells have been drilled in the region by an energy and water organization called the Salt River Project (SRP), and a few dozen wells in the East Salt River Valley shows distinct sediment facies from bottom to top (Fig. 1 and Fig. 4): (1) unit 1: basin fill deposits; (2) unit 2: ancestral Salt River deposit; and (3) unit 3: massive fine sand and silt deposit. A sharp contact between ancestral Salt River deposits and underlying basin-fill deposits, showing significantly different mineralogy (Fig. 4), indicates sudden arrival of Salt River in the East Salt River Valley. The timing of gravel burial is 836ka (at 27 - 30m in well log of Fig. 4), interpreted by a maximum burial age (Y. B. Seong, personal communication), which presents the maximum time limit of the deposition of the unit 3. Given the temporal constraint, it is reasonable that the interpretation of the uppermost fine sand and silt unit of the drilled wells assists to reconstruct paleoenvironment in the study area, from ~ 836ka to present.

The hypothesis to explain the transport and deposition processes of the uppermost fine sand and silt unit is fluvial-aeolian interactions. In other words, windblown sands and silts began to accumulate, deflated from the Gila River channel and ancestral Salt River channel that used to flow southward and then probably westward

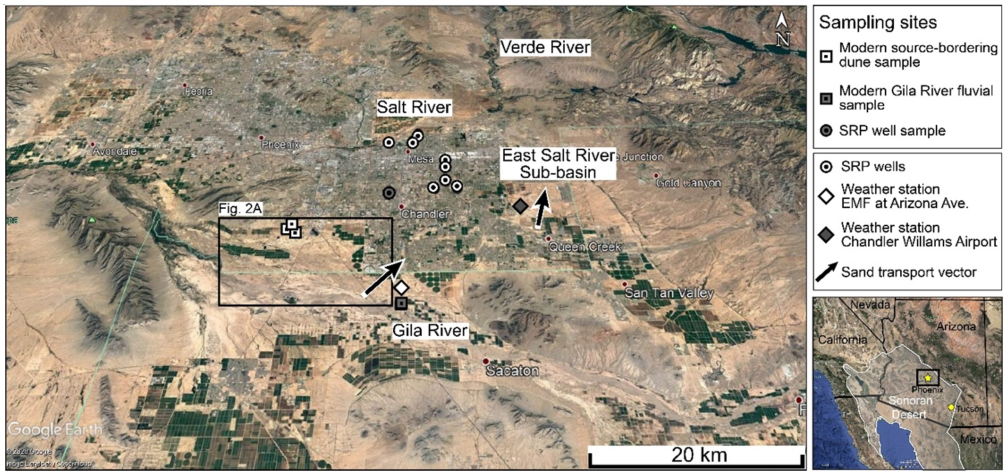

Fig. 1. Map of the Phoenix Metropolitan Area

* The map shows the locations of source-bordering dune and sand sheets near Gila River, SRP wells that have massive fine sand and silt deposit at the top (~ 40m), weather stations and sampling sites.

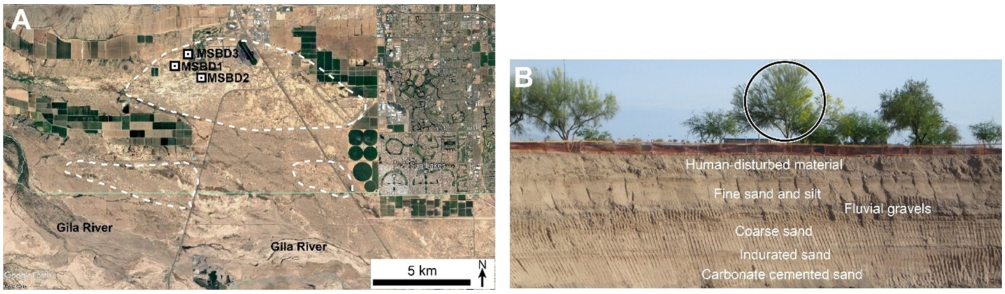

Fig. 2. Gila River Source-bordering Dunes and an Excavation Exposed the Mixed Fluvial and Aeolian Deposit

* (A) Source-bordering dunes near the Gila River in the southern part of the Phoenix Metropolitan area. MSBD refers samples collected from modern source-bordering dunes near the Gila River. Distinct dune forms are well-developed in areas denoted by the dashed lines, but a sand sheet covers the land between these areas; (B) An excavation exposed the mixed fluvial and aeolian deposit located between the Salt and the Gila Rivers in metropolitan Phoenix, Arizona, USA. Some fluvial gravels buried by overlying fine sand and silt unit provide evidence of both fluvial and aeolian transport. Note a 4-m tall Paloverde tree for scale.

around the south side of South Mountain during dry seasons (Dorn *et al.*, 2020; Skotnicki and DePonty, 2020; Skotnicki *et al.*, 2020) (Fig. 1). The purpose of this study is to reconstruct paleoenvironment and to understand the processes of transport and deposition (e.g. Hong, 2018; Oh, 2018; Jung and Park, 2019) of the paleo-fine sand and silt deposits in the uppermost layer of the drilled well-logs using modern analogues. To achieve the purpose: (1) The regional aeolian sediment drift potential (DP) based on Fryberger (1979) model is analyzed from local winds data to understand the development of source-bordering dunes and sand sheets near the Gila River (Fig. 1). (2) The analyses of grain size distributions and grain shape parameters from modern Gila River source-bordering dune sediments and Gila River fluvial sediments as well as the fine sand and silt deposits in the uppermost layer of the drilled well-log were performed to understand the paleoenvironments and processes affecting the development of the fine sand and silt deposits found in wells throughout the region (Fig. 3).

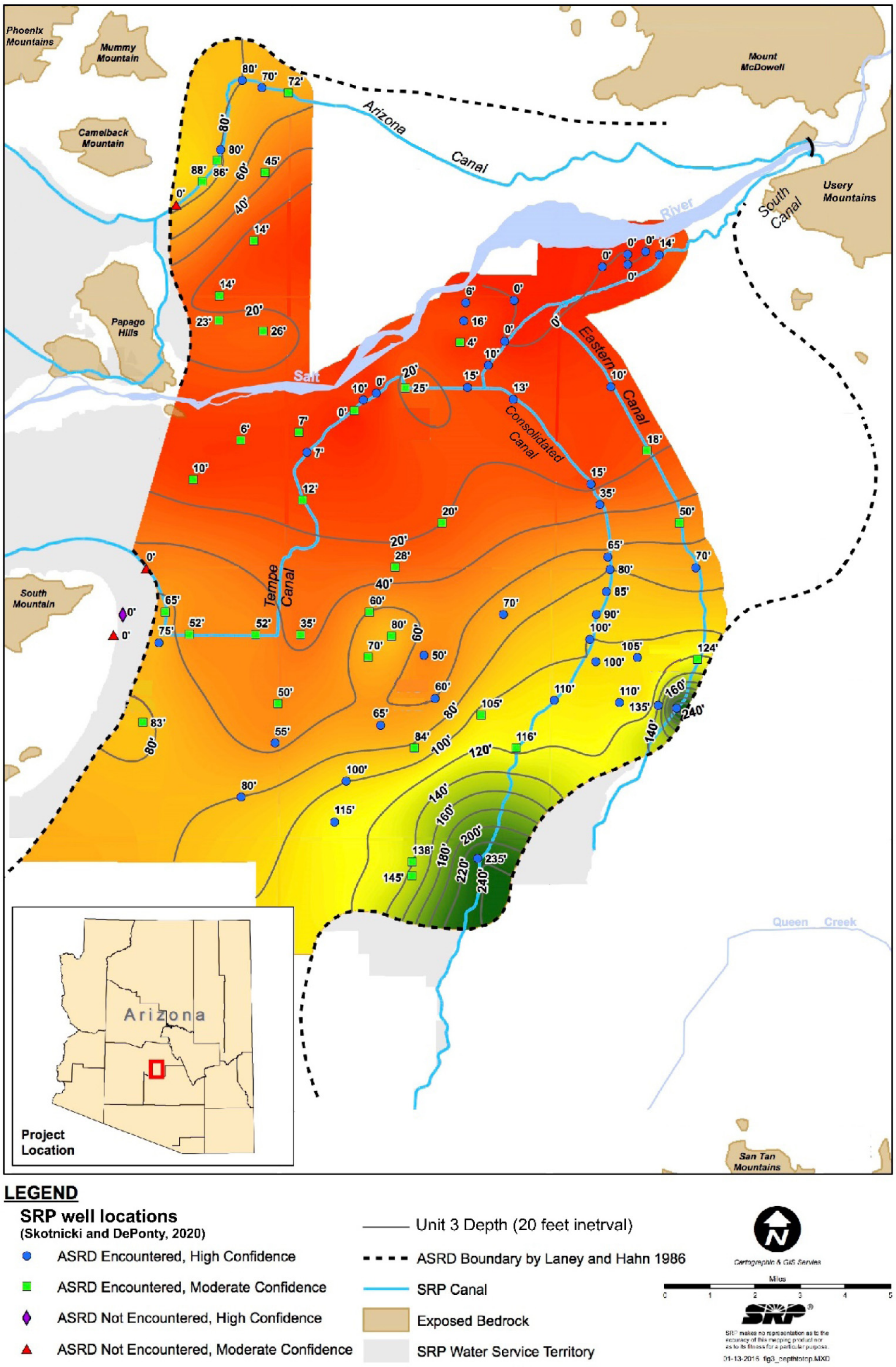

Fig. 3. Contour Map Showing the Depth of Paleo-massive Fine Sand and Silt Deposit (in feet)

* The map was generated from SRP wells data (Skotnicki and DePonty, 2020). ASRD stands for ancestral Salt River deposit. Courtesy of Skotnicki and DePonty (2020).

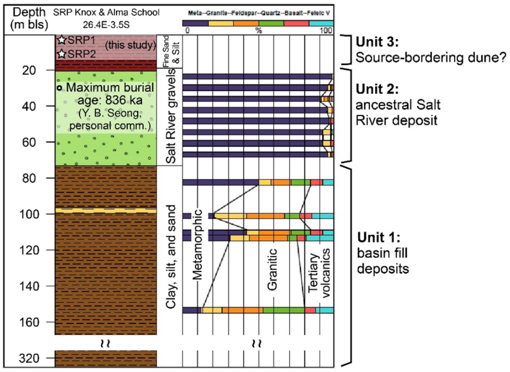

Fig. 4. Sedimentary Log of Sampled SRP Well and Sampling Depth

* The location of SRP well is shown in Figure 1. Sampling depth of SRP1 is 1.5 - 4.5m and SRP2 is 9 - 12m below surface. Note that maximum burial age of ancestral Salt River Deposit (ASRD) underlying the massive fine sand and silt deposit exists, which pre-dates the overlying unit. Courtesy of Skotnicki and DePonty (2020).

II. Materials and Methods

1. Regional Aeolian Sediment Drift Potential

The potential of local winds to transport fluvial sediments and deposited to Gila River source-bordering dune fields is estimated based on sediment drift rose developed by Fryberger (1979) using wind speed and direction data collected from Chandler Williams Airport station nearly over 80 years and from East Maricopa Floodway (EMF) at Arizona Ave. station in 2019 (Fig. 1). The 'Fryberger method' calculates the drift potentials (DPs) for all wind speed-direction categories (e.g., 10°, 11.25 - 14.4m/s) and sums up the DPs for each direction sector (e.g. 10°, 20°, 30°... 360°), then analyzes a resultant drift direction (RDD) and resultant drift potential (RDP) vector to show a general trend of sediment transport. In the calculation of DP, the frequency of winds above a transport threshold is involved, that based on following equation modified from Lettau and Lettau (1978):

$$Q \propto V^2(V - V_t) \times t \qquad (1)$$

Where Q is the sediment drift potential in vector units (VU), V is average wind velocity at 10m height in knots, V_t is the threshold velocity at the same height (2.7m/s in this case), and t is the time period expressed as a percentage. The net direction and quantity of sediment drift, RDD and RDP, can be calculated from vector analysis following the calculated DP values for all wind speed-direction classes. To minimize inherent frequency and magnitude biases in the model, the wind speeds were grouped into 36-point (10s of degree) classes (Pearce and Walker, 2005).

2. Grain Size and Shape Analyses and Statistical Tests

Two sediment samples from one SRP drilled well site (Fig. 1) were obtained with different depth intervals (Fig. 4) (SRP1: 1.5 - 4.5m and SRP2: 9 - 12m from the surface), and three modern source-bordering dune samples were collected from dune fields near the Gila River Casino (MSBD1 to 3), and one modern fluvial sediment sample was collected from the Gila River (MGR1) (Fig. 5). The MSBD and MGR sediment samples were collected from 10cm depth below the surface in the field. All samples were treated with acetic acid to remove organic materials and calcium carbonate, washed with distilled water several times and then dried. Grain size studies could provide helpful information on their depositional settings (e.g. Kim *et al.*, 2012; Rajganapathi *et al.*, 2013; Kim and Shin, 2014). In this study, grain size distribution was used to analyze the grain size parameters (mean, sorting, skewness, and kurtosis) of each sample. All the samples were sieved using the sieves stacked at 1/4φ Wentworth class size in a Ro-Tap sieve shaker for 10 minutes, and each sieve fraction was weighed with an electronic balance. GRADISTAT version 8 (Blott and Pye, 2001) was exploited to calculate the grain size parameters suggested by Folk and Ward (1957) and generated graphs of grain size distribution for each sample.

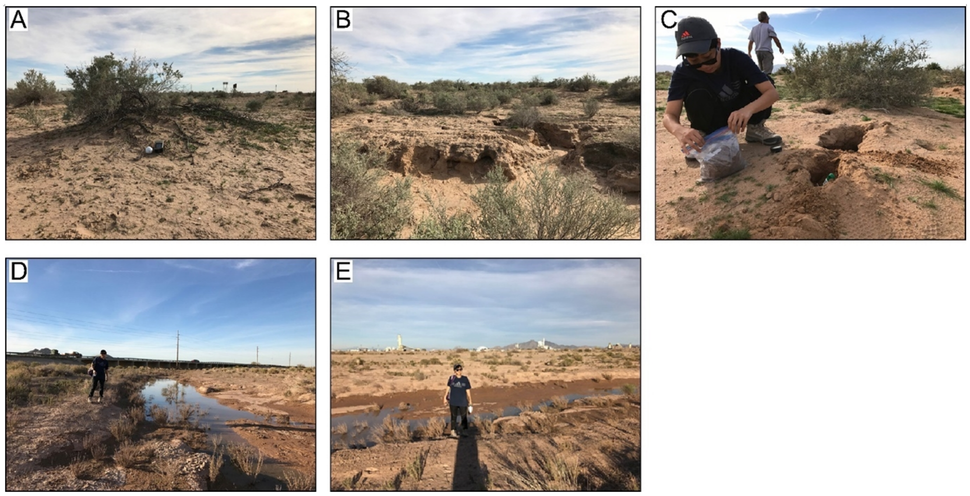

Fig. 5. Photographs of Collecting Samples around the Study Area.

* (A - C) Modern source-bordering aeolian dune fields near the Gila River where sediment samples (MSBD1, MSBD2 and MSBD3) were collected; (D - E) Gila River where fluvial sediment sample (MGR 1) was collected.

Grain shape analysis was also conducted to quantify the shape of grains using the grain shape descriptors in the ImageJ software (Table 1, Fig. 6). Eamer *et al.* (2017) presented a new method to differentiate the mechanism of transport for sandy deposits using an inexpensive and easily obtainable equipment with ImageJ software. The method is based on the effect of shape sorting that winds preferentially transport the sand grains with more spherical and rounded in shape (Mazzullo *et al.*, 1986). Eamer *et al.* (2017) examined the grain shape parameters of nearly 6000 grains from Calvert Island in Vancouver, Canada and indicated that grain solidity was the most noticeable parameters to differentiate aeolian and littoral sediments with an 86% success rate of prediction, and their classification of transport mechanism based on solidity matched 76%, suggesting a possible approach to determine the transport mechanism of sandy deposits between aeolian and littoral or fluvial sediments. In this study, the quartz grains from 3φ to 1.5φ grain-size classes of sample MSBD2, MGR1, and SRP1 were selected to analyze the grain shape parameters after the observation of grain surface textures and roundness with scanning electron microscopy (SEM). The most diagnostic features of a grain under fluvial environment are mechanical V-shaped etch patterns or depressions due to water abrasion process, while relatively weaker wind abrasion causes impacts between grains which produce upturned plates on the fractured portion or more rounded grains instead of etching (Krinsley and Doornkamp, 1973; Chakroun *et al.*, 2009). Based on the qualitative examination using SEM, MSBD2, MGR1, and SRP1 were selected as a representative sample for each environment. The sample size of each 1/4φ size class is 60. The images from each 1/4φ size class were imported into the ImageJ software to analyze the grain shape descriptors, including circularity, aspect ratio, roundness, and solidity (Fig. 6).

One-way analysis of variance (ANOVA) statistical tests were performed following the analyses of grain size and shape, to obtain parameters that assist to distinguish transport mechanism of the samples. A null hypothesis of the ANOVA tests was the parameters of two tested sample groups are drawn from the same population, which indicates the two samples have no statistically significant differences. First, Gila River source-bordering dune (MSBD) and fluvial (MGR) samples were statistically tested to find statistically significant parameters. Then statistical tests were conducted between paleo-massive

Table 1. The Definition and Equation of Grain Shape Descriptors

	Circularity	Aspect Ratio	Roundness	Solidity
Definition	Two-dimensional sphericity, ranging from 0 to 1 (Wadell, 1932; Krumbein, 1941)	The degree of elongation of particle in two dimensions (Eamer *et al.*, 2017)	Similar to circularity, but use major axis rather perimeter (Wadell, 1932), resulting in ignorance of irregular borders (Eamer *et al.*, 2017)	The irregularity of the border (Eamer *et al.*, 2017)
Equation	$4\pi\left(\frac{Area}{[Perimeter]^2}\right)$	$\frac{Major\ Axis}{Minor\ Axis}$	$4\left(\frac{Area}{\pi[Major\ Axis]^2}\right)$	$\frac{Area}{Convex\ Area}$

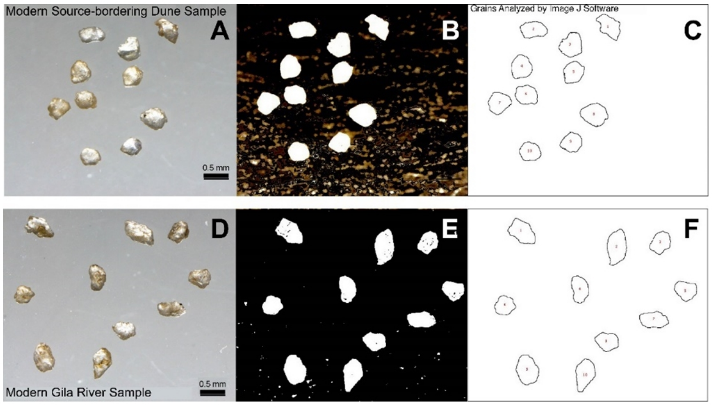

Fig. 6. The Process of Grain Shape Parameters Analysis

* Grain shape parameters analysis of modern source-bordering dune (A - C) and Gila River sediment sample (D - F) using the ImageJ software. The image of grains are first taken by light microscopy (A, D), then subject to digital image processing by ImageJ software (B, E), and then the recognized grain perimeter was used to generate grain shape parameters (C, F).

fine sand and silt deposit samples in SRP well (SRP) and MSBD or MGR sample to identify transport and depositional mechanism of the paleo-massive fine sand and silt deposit. ANOVA tests for grain shape descriptors were conducted via these steps: (1) seven grain size fraction of modern Gila River source-bordering dune (MSBD) and fluvial (MGR) samples were statistically tested to find statistically significant grain shape parameters. The reason why the samples were classified with the grain size is because coarser fraction could better reflect the transport mechanism. The fine fractions of the MGR sample could be aeolian inputs, so that whole sample analysis may serve to obscure the differences between the two samples; (2) Select the fractions that shows statistically significant differences between the two samples; and (3) Conduct statistical tests to the selected fractions of SRP and MSBD/MGR samples to identify transport and depositional mechanism of the paleo-massive fine sand and silt deposit.

III. Results

1. Regional Aeolian Sediment Drift Potential

Fig. 7 shows the wind rose of Chandler Williams Airport station and EMF at Arizona Ave. station. The threshold wind velocity to transport was 2.7m/s, the directions of winds with more than 2.7m/s at Chandler Williams Airport station are from ESE, SE, W, and E sector (Fig. 7A). At Arizona Ave. station, the direction of winds above the threshold velocity was mainly from SW sector (Fig. 7B). The sand drift potential values are shown in Fig. 7C and 7D. At Chandler Williams Airport

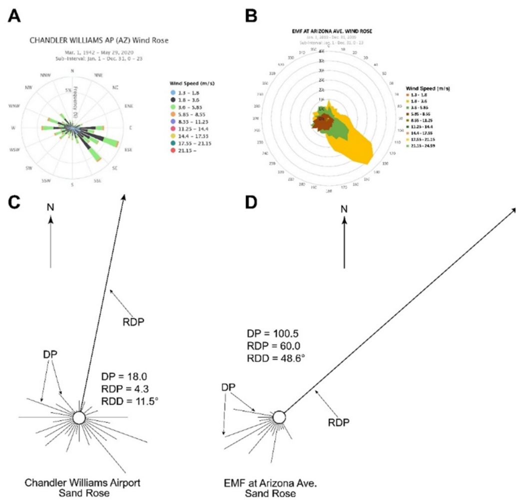

Fig. 7. Wind Rose and Sediment Drift Rose

* Wind rose was generated with cli-MATE (Midwestern Regional Climate Center application tools environment).

station, the DP values are 18 and the RDD is 11.5° (Fig. 7C), while the DP values are 100.5 and the RDD is 48.6° (Fig. 7D). Both regions are under low-energy environment (DP < 200 VU), based on the Fryberger (1979)'s classification of wind energy environments derived from more than one hundred of wind data sheets in global sand seas ranged from 80 to 489 VU (Bullard, 1997).

2. Grain Size Analysis

The mean grain size of SRP, MSBD and MGR sediment samples are 176 - 190μm (2.4 - 2.5φ), 155 - 208μm (2.6 - 2.7φ), and 503μm (1.0φ), respectively (Table 2). MGR sample is coarse skewed, but MSBD and SRP samples are relatively fine skewed (Figs. 8 and 9). The leptokurtic kurtosis of MGR 1 shows that the their frequency distribution graph has light-tailed relative to a normal distribution and the frequencies are concentrated in coarse fraction with the negative skewness, while the kurtosis of MSBD and SRP samples are platykurtic to mesokurtic indicating that their frequencies are relatively evenly distributed over the grain sizes (Table 2, Fig. 9).

Table 2. Grain-size Summary Statistics

Sample	Mean/Median grain size (μm)	Sorting	Skewness	Kurtosis
SRP1	176.3/174.7 (Fine Sand)	1.864 (Moderately Sorted)	0.049 (Symmetrical)	0.831 (Platykurtic)
SRP2	190.4/169.6 (Fine Sand)	2.181 (Poorly Sorted)	0.251 (Fine Skewed)	0.920 (Mesokurtic)
MSBD1	160.5/149.4 (Fine Sand)	1.944 (Moderately Sorted)	0.185 (Fine Skewed)	0.781 (Platykurtic)
MSBD2	154.8/148.2 (Fine Sand)	1.850 (Moderately Sorted)	0.157 (Fine Skewed)	0.929 (Mesokurtic)
MSBD3	208.4/214.7 (Fine Sand)	1.765 (Moderately Sorted)	-0.068 (Symmetrical)	1.035 (Mesokurtic)
MGR1	503.3/513.1 (Coarse Sand)	1.828 (Moderately Sorted)	-0.139 (Coarse Skewed)	1.140 (Leptokurtic)

* Descriptive terminology is modified from Krumbein and Pettijohn (1938) and Folk and Ward (1957).

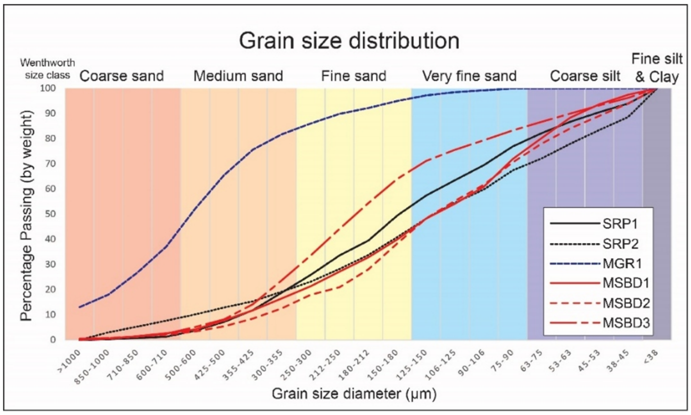

Fig. 8. A Graph Showing the Cumulative Grain-size Distribution of Analyzed Samples

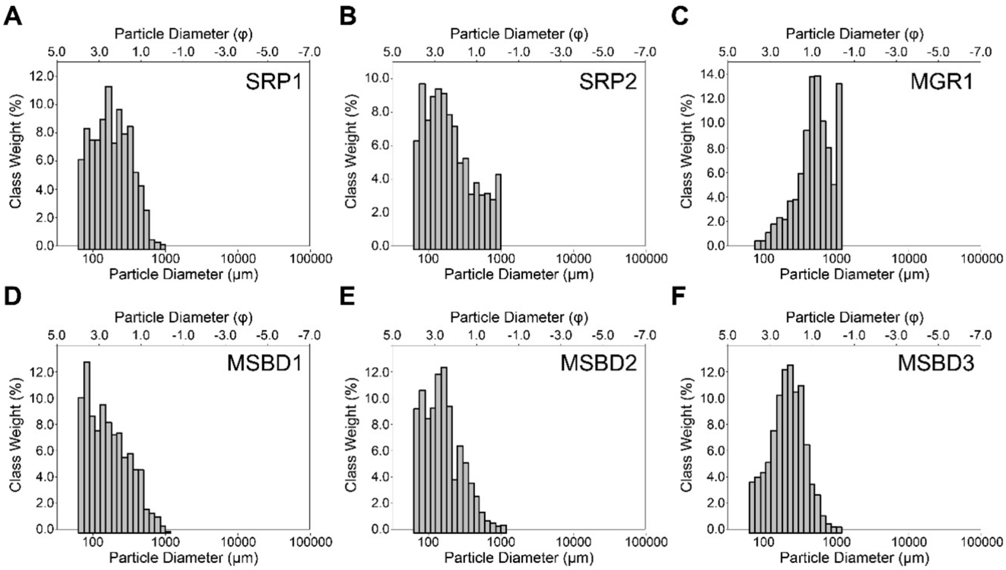

Fig. 9. Logarithmic Frequency Plot of each Sample

Table 3. Results of One-way ANOVA Statistical Test

Samples	Mean	Sorting	Skewness	Kurtosis
MSBD/MGR	Y (0.011)	N (0.831)	N (0.287)	N (0.266)
SRP/MSBD	N (0.723)	N (0.300)	N (0.678)	N (0.721)
SRP/MGR	Y (0.024)	N (0.608)	N (0.347)	N (0.181)

* Y = statistically different ($p < 0.05$), N = not statistically different, and significance value (*p*-value) in brackets.

The sorting of all samples are poor or moderate (Table 2). The ANOVA statistical tests show statistical difference at the 95% confidence level. The mean grain size of MGR shows a statistically significant differences with the mean grain size of MSBD sediments (p = 0.01), and SRP sediments (p = 0.02) (Table 3). Other grain size parameters (sorting, skewness, and Kurtosis) did not show a statistical difference at the 95% confidence level (Table 3).

3. Grain Shape Analysis

Among the four grain shape descriptors, aspect ratio and roundness are likely to be better descriptors to distinguish transport processes of modern Gila River source-bordering dune and fluvial sediments (Table 4). The result of grain shape analysis shows that the MSBD samples have a higher roundness (0.78 - 0.79) and lower aspect ratio (1.29 - 1.30) than MGR sample which shows 0.70 - 0.72 in roundness and 1.45 - 1.50 in aspect ratio. Eamer *et al.* (2017) reported solidity is the most noticeable parameters to differentiate aeolian and littoral sediments, but it is not a statistically significant parameter in this study. Rather, the higher roundness of MSBD samples is consistent with the observations of Mazzullo *et al.* (1986). For further analysis, coarser fraction grains (1.5φ and 1.75φ) were selected, since the coarser fraction grains of MSBD and MGR samples show more statistically significant difference in most of the grain shape descriptors than the finer fraction grains (2.75φ and 3φ) (Table 4). Additionally, 2.5φ sample was selected for the purpose of comparison.

The results of one-way ANOVA statistical test for MGR1 and SRP1 sample are represented in Table 5, and Table 6 shows the results of the one-way ANOVA

Table 4. Results of One-way ANOVA Statistical Test for MSBD2 and MGR1 Sample

D (μm)	N	Circularity	Aspect Ratio		Roundness		Solidity
			Mean (MSBD2, MGR1)	Difference?	Mean (MSBD2, MGR1)	Difference?	
350 (1.5φ)	60	Y (0.009)	1.290, 1.495	Y (0.015)	0.791, 0.704	Y (0.012)	N (0.543)
300 (1.75φ)	60	N (0.634)	1.302, 1.463	Y (0.034)	0.781, 0.716	Y (0.044)	Y (0.011)
250 (2φ)	60	N (0.212)	1.280, 1.411	Y (0.025)	0.794, 0.730	Y (0.032)	N (0.716)
210 (2.25φ)	60	N (0.394)	1.239, 1.531	Y (0.000)	0.819, 0.677	Y (0.000)	N (0.292)
177 (2.5φ)	60	N (0.970)	1.293,1.456	Y (0.017)	0.782, 0.719	Y (0.045)	N (0.678)
149 (2.75φ)	60	N (0.790)	1.298, 1.369	N (0.155)	0.784, 0.746	N (0.160)	N (0.101)
125 (3φ)	61	N (0.441)	1.424, 1.579	N (0.092)	0.721, 0.671	N (0.157)	N (0.878)

* D is the grain diameters, and N is the number of grains analyzed. The bracket next to the decision (Y or N) indicates the p-value. The mean aspect ratio and roundness for MSBD2 and MGR1 are presented in the left-hand column.

Table 5. Results of one-way ANOVA statistical test for MGR1 and SRP1 sample

D (μm)	N	Circularity	Aspect Ratio		Roundness		Solidity
			Mean (MGR1, SRP1)	Difference?	Mean (MGR1, SRP1)	Difference?	
350 (1.5φ)	60	Y (0.000)	1.495, 1.332	Y (0.050)	0.704, 0.766	N (0.066)	Y (0.000)
300 (1.75φ)	60	Y (0.000)	1.463, 1.346	N (0.132)	0.716, 0.759	N (0.199)	Y (0.002)
177 (2.5φ)	60	N (0.412)	1.455, 1.321	N (0.071)	0.718, 0.775	N (0.109)	N (0.072)

Table 6. Results of one-way ANOVA statistical test for MSBD2 and SRP1 sample

D (μm)	N	Circularity	Aspect Ratio		Roundness		Solidity
			Mean (MSBD2, SRP1)	Difference?	Mean (MSBD2, SRP1)	Difference?	
350 (1.5φ)	60	Y (0.000)	1.290, 1.332	N (0.419)	0.790, 0.766	N (0.377)	Y (0.000)
300 (1.75φ)	60	Y (0.000)	1.302, 1.346	N (0.374)	0.780, 0.759	N (0.430)	Y (0.000)
177 (2.5φ)	60	N (0.310)	1.293, 1.321	N (0.542)	0.782, 0.775	N (0.789)	N (0.245)

statistical test for MSBD2 and SRP1 sample. Some key observations follow:

1) The finer fraction grain (2.5φ) was not an ideal grain size to find parameters that assist to differentiate samples statistically. In other words, the four grain shape descriptors were not effective parameters to distinguish MGR1/SRP1 and MSBD2/SRP1 sample.
2) Circularity and solidity were not useful parameters to find similarity between SRP and MGR sample or between SRP and MSBD sample. The results of one-way ANOVA statistical test for the circularity and solidity of the coarser fraction grains (1.5φ and 1.75φ) showed that MGR1 and SRP1 are statistically different (Table 5), but also MSBD2 and SRP1 are statistically different (Table 6). Thus, to identify the transport mechanism of SRP1 sample using the circularity and solidity is obscure.
3) The useful parameters that effectively distinguish the MGR and MSBD sample was aspect ratio and roundness of the coarser fraction grains (Table 4), but only aspect ratio partly worked to find similarity between SRP and MGR sample or between SRP and MSBD sample. The aspect ratio of the 1.5φ grains showed that MGR1 and SRP1 are statistically different (Table 5), but MSBD2 and SRP1 are not statistically different (Table 6).

IV. Discussion

The hypothesis in this study to explain the transport and deposition processes of the uppermost fine sand

and silt deposits in the SRP well was fluvial-aeolian interactions, and the deposits were windblown deposits, deflated from the ancestral Salt River channel (Dorn *et al.*, 2020; Skotnicki and DePonty, 2020; Skotnicki *et al.*, 2020) and the Gila River channel during dry seasons that accumulated no later than 836 ka. Overall, the results of sediment drift potential, grain size distribution and shape analyses provide evidence to support the hypothesis. The modern Gila River dune fields has been formed by transported sediments from the upwind source area (floodplains or a fluvial sandbar of Gila River) towards the downwind dune fields (Fig. 1). The calculated resultant drift direction showed the strong evidence that Gila River dune fields are source-bordering dune, which is consistent with the interpretations of Wright *et al.* (2011) that eolian sands in the Gila River dune fields (~ 2m depth) are related with flow variability of the Gila River in the past 2000 years. The paleo-fine sand and silt deposits in the SRP well (~ 20m bls) could be deposited through similar processes if the SRP deposits have similar characteristics with the modern source-bordering dune sediments near Gila River. The statistical tests of grain size distribution and grain shapes supported the paleo-deposits in SRP drilled well likely experienced similar mechanism of transport to the sediments in the modern Gila River source-bordering dunes. The mean grain size and the aspect ratio were the most distinguishable characteristic between the modern Gila River source-bordering dune and fluvial sediments, which successfully assists to interpret that the SRP paleo-deposits is likely experienced similar mechanism of transport to the sediments in the modern Gila River source-bordering dunes, showing no statistical difference between the SRP and MSBD samples. Since the entrainment of sediment grain largely depends on the specific shear stress acting on the bed and its resisting force, weaker drag force of winds than waters may lead to selectively transport of smaller, lighter grains. Fortunately, grain size distribution was a useful indicator to distinguish the mechanism of transport in this study, but it does not well reflect the mechanism of transport in some cases occurred over relatively short distances (Eamer *et al.*, 2017). Rather, shape sorting can occur over relatively short distances, because it requires less shear stress for entrainment of grain (Eamer *et al.*, 2017) and thus grain shape parameters could discern the mechanism of transport more effectively. In this study, the aspect ratio decreased away from the source such as in MSBD and SRP samples, as expected for grain rounding processes with transport distance (Szabó *et al.*, 2015).

The deposition of the paleo-fine sand and silt deposits throughout the region (Fig. 3) may be related with the change of regional climates. There is ample evidence that the Sonoran Desert was more humid and cooler during the late Pleistocene. Pollen records in northern Baja California from 44 to 13 ka (Lozano-García *et al.*, 2002) and packrat midden studies in the Sonoran Desert in the same late Pleistocene time range (van Devender, 1990; Allen *et al.*, 1998; McAuliffe and van Devender, 1998) indicates that the region was not a desert until the Holocene. Thus, more extensive vegetation covered in the region in the last glacial period and perhaps previous glacial cycles, based on the paleo-climate evidence (Jeong *et al.*, 2018). The possibility that fluvial sediment deposits in vegetated channels are transported by aeolian systems are likely low, compared to the fluvial deposits on unvegetated or open area (Bullard and Livingstone, 2002). Historical data supports this hypothesis that the AD 1200 and 1500 eolian events occurred in the Gila River dune fields are consistent with the timing of the megadroughts (Cook *et al.*, 2007; Stahle *et al.*, 2007) in the southwestern United States (Wright *et al.*, 2011). Thus, when the region became drier and hotter, fine sand, silt and clays deflated from the ancestral Salt River and Gila River channel would have been deposited nearby, and remained a distinct layer throughout the region (Fig. 3) that represents a wind-blown deposit derived from the floodplains of the ancestral Salt and Gila Rivers.

In Korea, there has been a debate for the last 30 years over whether the loess-like sediments observed throughout Korea were transported from the far-distant Chinese

Loess Plateau and peripheral areas (Park *et al.*, 2007; Yoon *et al.*, 2007; Hwang *et al.*, 2009) or locally transported from nearby floodplains or from exposed fine materials in the Yellow Sea (Oh and Kim, 1994; Kim, 2007). The analysis of grain size distribution has been widely used to identify the provenance of sedimentary deposits or interpret paleoenvironment (e.g. Kim *et al.*, 2012; Kim and Shin, 2014), but grain shape analysis was rarely used (e.g. Choi, 2020). Given the advantage of grain shape analysis that effectively reflects the mechanism of transport occurred over relatively short distance (Eamer *et al.*, 2017), it may provide a new insight to solve the issue associated with the provenance of Korean loess-like sediments.

V. Conclusion

The purpose of this study was to reconstruct paleoenvironment and to understand the processes of transport and deposition of the fine sand and silt deposits using modern analogues. This was accomplished via the identification of the fine sand and silt deposits by comparison with modern source-bordering dune sediments and modern fluvial sediments using the analyses of grain size distribution and grain shape parameters. The deposition of the paleo-fine sand and silt deposits throughout the Phoenix metropolitan area in north-central Sonoran Desert may be related with the change of regional climates. Unlike grain size distribution, grain shape parameters may better reflect the mechanism of transport that even grains traveled over short distance. Given the advantage, the grain shape analysis may provide a new insight to solve the issue associated with the provenance of Korean loess-like sediments whether it was originated from far-distant the Chinese Loess Plateau and peripheral areas (Park *et al.*, 2007; Yoon *et al.*, 2007; Hwang *et al.*, 2009) or from nearby floodplains of local river or from exposed fine materials in the Yellow Sea (Oh and Kim, 1994; Kim, 2007).

Bullard and Livingstone (2002) argued in their review paper that some key goals in future research would be "to understand the responses of areas dominated by [aeolian-fluvial] interactions to climate changes and the spatial and temporal scales at which these interactions take place (Bullard and Livingstone, 2002: 15)." This paper certainly demonstrated that the extensive paleo-fine sand and silt deposits observed throughout the Sonoran Desert is likely wind-blown deposit derived from the floodplains of the channels nearby, and probably started to accumulate when the climate of the region shifted from humid and cooler during the late Pleistocene to the drier and hotter after the last glacial period. Relatively little is known about the landscape history and geomorphic processes that has been formed the landscape of the Sonoran Desert (e.g. Spencer and Reynolds, 1989; Seong *et al.*, 2016a; Seong *et al.*, 2016b; Jeong *et al.*, 2018; Jeong and Dorn, 2019; Jeong, 2019; 2020; Oh *et al.* 2020; Skotnicki *et al.*, 2020). In particular, the interactions between aeolian and fluvial process has rarely studied despite their efficacy to shape landscape in dryland. The establishment of modern analogues in this study successfully assisted the reconstruction of paleoenvironment in the region and filled the research gap.

Acknowledgement

I would like to thank Suet Yi Cheung of the North Carolina State University for field and lab assistance as well as for valuable feedback in discussions. I would like to thank Ave Choi for support. I would like to thank Steve Skotnicki and Jersy DePonty for allowing access to maps that are in press. I would like to thank Ian Walker and Ronald Dorn of the Arizona State University and Yeong Bae Seong of Korea University for valuable feedback in discussions. I thank Steve Skotnicki for providing maps, well log and mineralogical analyses during the in-press stage of a manuscript. I also thank anonymous reviewers for their helpful comments on how to improve this paper.

References

Alizai, A., Carter, A., Clift, P.D., VanLaningham, S., Williams, J.C., and Kumar, R., 2011, Sediment provenance, reworking and transport processes in the Indus River by U–Pb dating of detrital zircon grains, *Global and Planetary Change*, 76, 33-55.

Allen, C., Swetnam, T., and Betancourt, J., 1998, Landscape changes in the southwestern United States: Techniques, long-term data sets, and trends, in Sisk, T.D., ed., *Perspectives on the Land-Use History of North America: A Context for Understanding Our Changing Environment*, Fort Collins, CO: U.S. Geological Survey, 71-84.

Bagnold, R.A., 1941, *The Physics of Blown Sand and Desert Dunes*, London: Methuen.

Belnap, J., Munson, S.M., and Field, J. P., 2011, Aeolian and fluvial processes in dryland regions: The need for integrated studies, *Ecohydrology*, 4(5), 615-622.

Blott, S.J. and Pye, K., 2001, GRADISTAT: A grain size distribution and statistics package for the analysis of unconsolidated sediments, *Earth Surface Processes and Landforms*, 26(11), 1237-1248.

Bullard, J.E., 1997, A note on the use of the "Fryberger method" for evaluating potential sand transport by wind, *Journal of Sedimentary Research*, 67(3), 499-501.

Bullard, J.E. and Livingstone, I., 2002, Interactions between aeolian and fluvial systems in dryland environments, *Area*, 34(1), 8-16.

Chakroun, A., Miskovsky, J.C., and Zaghbib-Turki, D., 2009, Quartz grain surface features in environmental determination of aeolian Quaternary deposits in northeastern Tunisia, *Mineralogical Magazine*, 73(4), 607-614.

Choi, K.H., 2020, Grain Size Analysis Using Morphological Properties of Grain, *Journal of the Korean Geomorphological Association*, 27(2), 19-28 (in Korean).

cli-MATE, *Midwestern Regional Climate Center, Illinois State Water Survey*, Prairie Research Institute, University of Illinois at Urbana-Champaign (http://mrcc.illinois.edu/CLIMATE).

Cook, E.R., Seager, R., Cane, M.A., and Stahle, D.W., 2007, North American drought: Reconstructions, causes, and consequences. *Earth Science Reviews*, 81, 93-134.

Dorn, R. I., Skotnicki, S. J., Wittman, A., and Van Soest, M., 2020, Provenance in drainage integration research: Case studies from the Phoenix metropolitan area, south-central Arizona, *Geomorphology* (in press).

Eamer, J.B.R., Shugar, D.H., Walker, I.J., Lian, O.B., and Neudorf, C.M., 2017, Distinguishing depositional setting for sandy deposits in coastal landscapes using grain shape, *Journal of Sedimentary Research*, 87(1), 1-11.

Folk, R.L. and Ward, W.C., 1957, Brazos River bar: A study in the significance of grain size parameters, *Journal of Sedimentary Petrology*, 27(1), 3-26.

Fryberger, S.G., 1979, Dune forms and wind regime, in McKee, E.D., ed., *A Study of Global Sand Seas, USGS Professional Paper,* Vol. 1052, Washington D.C.: US Geological Survey and United States National Aeronautics and Space Administration, 137-169.

Hong, S., 2018, A review on OSL age results of marine terrace deposits in Korea, *Journal of the Association of Korean Geographers*, 7(2), 157-164 (in Korean).

Jeong, A., 2019, Sediment accumulation expectations for growing desert cities: A realistic desired outcome to be used in constructing appropriately sized sediment storage of flood control structures, *Environmental Research Letters*, 14(12), 125005 (https://doi.org/10.1088/1748-9326/ab30e5).

Jeong, A., 2020, Spatial analysis for detrital zircon provenance study: An initial study, *Journal of the Korean Geographical Society* (in press).

Jeong, A., Cheung, S.Y., Walker, I.J., and Dorn, R.I., 2018, Urban geomorphology of an arid city: Case study of Phoenix, Arizona, in Thornbush, M.J. and Allen, C.D., eds., *Urban Geomorphology, Landforms and Processes in Cities,* Cambridge, MA: Elsevier, 177-204.

Jeong, A. and Dorn, R.I., 2019, Soil erosion from urbanization processes in the Sonoran Desert, Arizona, USA, *Land Degradation & Development*, 30(2), 226-238.

Jung H.K. and Park, J.-H., 2019, Possibility of paleoclimatic environmental change and human influence around

Haman Seongsan Fortress, *Journal of the Association of Korean Geographers*, 8(1), 71-78 (in Korean).

Kim, J.Y., Yi, S.H., and Kim, J.W., 2012, A study on mountain stream type deposit at Suhang Valley in Odaecheon, *Journal of the Association of Korean Geographers*, 1(1), 75-90 (in Korean).

Kim, J.Y. and Shin, W.J., 2014, A study on the characteristic of sediment particles of glacial period in the Suip River, Yanggu, *Journal of the Association of Korean Geographers*, 3(1), 53-66 (in Korean).

Kim, Y.R., 2007, Properties of local loess of small basin in Charyong Ranges-Iljuk, Anseong City, Central Korea, *Journal of the Korean Geomorphological Association*, 14(2), 67-81 (in Korean).

Krinsley, D.H. and Smalley, I.J., 1972, Sand: The study of quartz sand in sediments provides much information about ancient geological environments, *American Scientist*, 60(3), 286-291.

Krinsley, D.H. and Doornkamp, J.C., 1973, *Atlas of Sand Grain Surface Textures*, Cambridge: Cambridge University Press.

Krumbein, W.C., 1941, Measurement and geological significance of shape and roundness of sedimentary particles, *Journal of Sedimentary Research*, 11(2), 64-72.

Krumbein, W.C. and Pettijohn, F.J., 1938, *Manual of Sedimentary Petrography*, New York: Appleton-Century-Crofts.

Laney, R.L. and Hahn, M.E., 1986, Hydrogeology of the eastern part of the Salt River Valley area, Maricopa and Pinal Counties, Arizona, in *US Geological Survey Water-Resources Investigations Report*, No. 86-4147 (4 sheets).

Lettau, K. and Lettau, H.H., 1978, Experimental and micrometeorological field studies on dune migration, in Lettau, K. and Lettau, H.H., eds., *Exploring the World's Driest Climate*, *IES Report*, Vol. 101, Madison, WI: University of Wisconsin Press, 110-147.

Lozano-García, M.S., Ortega-Guerrero, B., and Sosa-Nájera, S., 2002, Mid-to late-Wisconsin pollen record of San Felipe basin, Baja California, *Quaternary Research*, 58(1), 84-92.

Mazzullo, J.I.M., Sims, D., and Cunningham, D., 1986, The effects of eolian sorting and abrasion upon the shapes of fine quartz sand grains, *Journal of Sedimentary Research*, 56(1), 45-56.

McAuliffe, J.R. and van Devender, T.R., 1998, A 22,000-year record of vegetation change in the north-central Sonoran Desert, *Palaeogeography, Palaeoclimatology, Palaeoecology*, 141(3-4), 253-275.

Muhs, D.R., Reynolds, R.L., Been, J., and Skipp, G., 2003, Eolian sand transport pathways in the southwestern United States: Importance of the Colorado River and local sources, *Quaternary International*, 104(1), 3-18.

Oh, J.S., 2018, Discussion on the characteristics and formation age of the reddish-yellow semi-consolidation deposits, west coast of Korea: Comparison with the Ujeon coast deposits in Jeungdo, *Journal of the Association of Korean Geographers*, 7(1), 55-68 (in Korean).

Oh, J.S., Seong, Y.B., Larson, P.H., Hong, S.C., and Yu, B.Y., 2020, Asymmetric hillslope retreat revealed from talus flatirons on rock peak, San Tan Mountains, Arizona, United States: Assessing caprock lithology control on landscape evolution, *Annals of the American Association of Geographers*, 110(1), 98-119.

Oh, K-S. and Kim, N-S., 1994, Origin and post-depositional deformation of the superficial formations covering basalt plateau in Chungok area, *The Korean Journal of Quaternary Research*, 8(1), 43-68 (in Korean).

Page, K.J., 1971, Riverine source bordering sand dune, *Australian Geographer*, 11(6), 603-605.

Page, K.J., Dare-Edwards, A.J., Owens, J.W., Frazier, P.S., Kellett, J., and Price, D.M., 2001, TL chronology and stratigraphy of riverine source bordering sand dunes near Wagga Wagga, New South Wales, Australia, *Quaternary International*, 83, 187–193.

Park, C.S., Yoon, S.O., and Hwang, S.I., 2007, Results and discussion for loess research in Korea, *Journal of the Korean Geomorphological Association*, 14(4), 29-45 (in Korean).

Park, C.S., Yoon, S.O., and Hwang, S.I., 2014, Formative process and sedimentary environment of loess sediments around Mt. Bulhwa, Gangneung-si, South Korea, *Journal of the Korean Geomorphological*

Association, 21(3), 49-61 (in Korean).

Park, D.W., 1985, A study on the loessial red yellow soil of Hwangsan, Kimje county and Gamgok, Chungeup county of the south western coastal area of Korea, *Geography*, 20(2), 1-10 (in Korean).

Pearce, K.I. and Walker, I.J., 2005, Frequency and magnitude biases in the 'Fryberger' model, with implications for characterizing geomorphically effective winds, *Geomorphology*, 68(1-2), 39-55.

Rajganapathi, V.C., Jitheshkumar, N., Sundararajan, M., Bhat, K.H., and Velusamy, S., 2013, Grain size analysis and characterization of sedimentary environment along Thiruchendur coast, Tamilnadu, India, *Arabian Journal of Geosciences*, 6(12), 4717-4728.

Seong, Y.B., Dorn, R.I., and Yu, B.Y., 2016a, Evaluating the life expectancy of a desert pavement, *Earth-Science Reviews*, *162*, 129-154.

Seong, Y.B., Larson, P.H., Dorn, R.I., and Yu, B.Y., 2016b, Evaluating process domains in small arid granitic watersheds: Case study of Pima Wash, South Mountains, Sonoran Desert, USA, *Geomorphology*, *255*, 108-124.

Skotnicki, S.J., Seong, Y.B., Dorn, R.I., Larson, P.H., and DePonty, J., 2020, Drainage integration of the Salt and Verde Rivers in a Basin and Range extensional landscape, central Arizona, USA, *Geomorphology* (in press).

Skotnicki, S.J. and DePonty, J., 2020, Subsurface evidence for the initial integration of the Salt River, Arizona, using clast assembles of subsurface drill cuttings, *Geomorphology* (in press).

Spencer, J.E. and Reynolds, S.J., 1989, Middle tertiary tectonics of Arizona and adjacent areas, *Arizona Geological Society Digest,* 17, 539-574.

Stahle, D.W., Fye, F.K., Cook, E.R., and Griffin, R.D., 2007, Tree-ring reconstructed megadroughts over North America since AD 1300, *Climatic Change*, 83, 133-149.

Szabó, T., Domokos, G., Grotzinger, J.P., and Jerolmack, D.J., 2015, Reconstructing the transport history of pebbles on Mars, *Nature Communications*, *6*(1), 1-7.

van Devender, T.R., 1990, Late Quaternary vegetation and climate of the Sonoran Desert, United States and Mexico, in Betancourt, J.L., van Devender, T.R., and Martin, P.S., eds., *Packrat Middens: The Last 40,000 Years of Biotic Change*, Tucson, AZ: University of Arizona Press, 134–165.

Wadell, H., 1932, Volume, shape, and roundness of rock particles, *The Journal of Geology*, 40(5), 443-451.

Wright, D.K., Forman, S.L., Waters, M.R., and Ravesloot, J.C., 2011, Holocene eolian activation as a proxy for broad-scale landscape change on the Gila River Indian Community, Arizona, *Quaternary Research*, 76(1), 10-21.

Yoon, S.O., Park, C.S., Hwang, S.I., and Naruse, T., 2007, Weathering characteristics of loess-paleosol sequence at the Daecheon area, South Korea, *Journal of the Geological Society of Korea*, 43(3), 281-296 (in Korean).

Yoon, S.O., Park, C.S., and Hwang, S.I., 2012, The formation and characteristics of loess sediments during the last glacial period in the Eonyang area, Ulsan-si, Korea, *Journal of the Korean Geomorphological Association*, 20(3), 1-14 (in Korean).

Yoon, S.O., Park, C.S., and Hwang, S.I., 2013, Formation and sedimentary environment of loess-paleosol sequence in the Jincheon Basin, Chungbuk Province, Korea, *Journal of the Korean Geomorphological Association*, 20(3), 1-14 (in Korean).

Arizona State Climatologists office, https://azclimate.asu.edu

Correspondence : Ara Jeong, 145 Anam-ro, Seongbuk-gu, Seoul, Korea, Department of Geography Education, College of Education, Korea University (Email: ara0408@korea.ac.kr)

교신 : 정아라, 02841, 서울특별시 성북구 안암로 145, 고려대학교 사범대학 지리교육과(이메일: ara0408@korea.ac.kr)

투고접수일: 2020년 7월 17일
심사완료일: 2020년 7월 30일
게재확정일: 2020년 8월 4일